Double Space–Time Line Codes

Jingon Joung, *Senior Member, IEEE*,
Jihoon Choi, *Senior Member, IEEE*,
and Bang Chul Jung, *Senior Member, IEEE*

***Abstract*—In this paper, an $M \times 4$ double space-time line code (D-STLC) is designed for a system with M-transmit and four-receive antennas whose channel state information is available at the transmitter. By delivering two independent STLC data streams simultaneously, both spatial diversity and multiplexing gains are obtained, like a $4 \times M$ double space-time transmit diversity (DSTTD) system that transmits two space-time block coded data streams. It is analytically shown that the decoding signal-to-interference-plus-noise ratios of D-STLC and DSTTD are identical to each other, and furthermore, it is numerically verified that the proposed D-STLC significantly outperforms a conventional $M \times 4$ STLC scheme and other existing spatial-diversity and spatial-multiplexing schemes, such as precoded space-time block code and precoded spatial multiplexing, in terms of achievable rate and bit-error-rate performance as the signal-to-noise ratio and/or transmission data rate increase.**

***Index Terms*—Space-time line code, spatial diversity, spatial multiplexing, precoding, DSTTD, STBC.**

I. Introduction

Recently, a space-time line code (STLC) has been proposed in [1] as a dual transmission scheme of space-time block code (STBC) [2]–[5]. Basic antenna configurations of STLC and STBC are symmetric, e.g., a 1×2 STLC system that has the one-transmit antenna and two-receive antennas, as shown in Fig. 1(a), is symmetric with a 2×1 STBC system that has two-transmit antennas and one-receive antenna. Both 1×2 STLC and 2×1 STBC achieve full spatial-diversity gain with the order of two and full data rate, i.e., one symbol per transmission. Furthermore, they are symmetric for the channel state information (CSI): full CSI is assumed to be known only at the transmitter (Tx) for STLC, whereas only at the receiver (Rx) for STBC. Since the STLC encoding and decoding can be implemented by using a simple linear processing like the STBC, the STLC scheme has been applied to various communication systems in which CSI is available at the Tx, such as the massive multiple-input and multiple-output (MIMO) and multiuser systems [6], [7], two-way relay systems [8], [9], antenna shuffling systems [10], machine learning-based blind decoding systems [11], and physical-layer security systems [12]. The previous studies on STLC, however, have considered a single-data stream transmission for each Rx.

Manuscript received March 30, 2019; revised July 15, 2019, October 1, 2019, and November 27, 2019; accepted December 1, 2019. Date of publication December 9, 2019; date of current version February 12, 2020. This work was supported by the National Research Foundation of Korea (NRF) of the Korea Government (MSIT) under Grant 2018R1A4A1023826. The review of this article was coordinated by Prof. Y. L. Guan. *(Corresponding author: Jihoon Choi.)*

J. Joung is with the School of Electrical and Electronics Engineering, Chung-Ang University, Seoul 06974, South Korea (e-mail: jgjoung@cau.ac.kr).

J. Choi is with the School of Electronics and Information Engineering, Korea Aerospace University, Gyeonggi-do 10540, South Korea (e-mail: jihoon@kau.ac.kr).

B. C. Jung is with the Department of Electronics Engineering, Chungnam National University, Daejeon 34134, Korea (e-mail: bcjung@cnu.ac.kr).

Digital Object Identifier 10.1109/TVT.2019.2958666

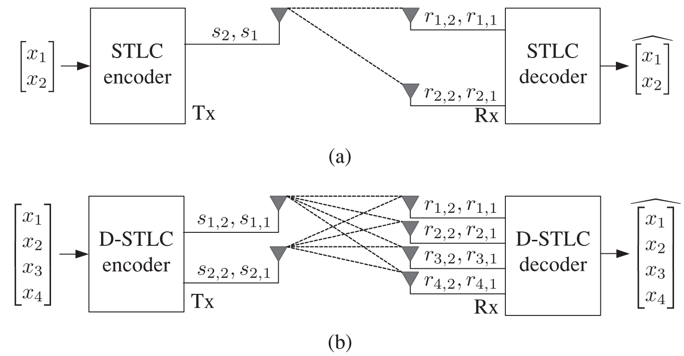

Fig. 1. STLC system models. (a) The conventional 1×2 STLC system [1], [6]–[11]. (b) The proposed $M \times 4$ D-STLC system when $M = 2$.

This paper considers an $M \times 4$ system with M-transmit and four-receive antennas. When the CSI is available at the Tx, STBC schemes combined with precoding have been investigated for limited feedback precoding [13], an optimal precoder design under CSI uncertainty [14], and linear precoding over correlated Rician channels [15]. The limited feedback precoding in [13] achieves diversity gain when the transmitter has more than two antennas, and the precoding schemes in [14] and [15] improve the performance of STBC under imperfect CSI and/or correlated channels. Moreover, these schemes require CSI at both Tx and Rx. In [16], precoded spatial multiplexing (SM) with channel inversion was proposed for multi-stream transmission with perfect CSI at a Tx, however, this method presents significant performance degradation due to noise enhancement.

On the other hand, 4×2 double space–time transmit diversity (DSTTD) schemes that can deliver two-multiplexed STBC signals simultaneously were proposed to increase the data rate of the STBC systems [17]–[20]. However, no such kind of rate enhancing schemes has been studied for the STLC systems so far.

In this paper, assuming that the CSI is available at the Tx, we propose a double STLC (D-STLC) that delivers two-STLC data streams through an $M \times 4$ channel of M-transmit and 4-receive antennas, where $M \geq 2$, as shown in Fig. 1(b) with $M = 2$. Sustaining the STLC decoding structure (i.e., received signal combining) at the Rx, a D-STLC precoding matrix is designed based on a minimum mean-square error (MMSE) criterion. Similar to the symmetry between STLC and STBC, the proposed $M \times 4$ D-STLC and the $4 \times M$ DSTTD schemes are perfectly symmetric for the antenna configuration and the CSI condition, and their signal-to-interference-plus-noise ratios (SINRs) are the same as each other. It is analytically shown that the decoding SINR of $M \times 4$ D-STLC is identical to that of $4 \times M$ DSTTD. From numerical results, it is verified that the proposed $M \times 4$ D-STLC system achieves better achievable rate and bit-error-rate (BER) performance than an existing single-stream $M \times 4$ STLC system, precoded STBC, and precoded SM systems, especially, as the signal-to-noise ratio (SNR) and/or transmission data rate increase.

Notations: Superscripts T, H, $*$, and -1 denote transposition, Hermitian transposition, complex conjugate, and inversion, respectively, for any scalar, vector, or matrix. The notation $|x|$, $\|\boldsymbol{x}\|$, and $\|\boldsymbol{X}\|_F$ denote the absolute value of x, the norm of vector $\boldsymbol{x}$, and the Frobenius-norm of matrix $\boldsymbol{X}$, respectively; $\boldsymbol{I}_m$ and $\boldsymbol{0}_m$ represent an m-by-m identity matrix and a zero matrix, respectively; $\mathrm{tr}(\boldsymbol{A})$ is a trace operation of matrix $\boldsymbol{A}$; $\boldsymbol{A}\otimes\boldsymbol{B}$ represents the Kronecker product of matrices $\boldsymbol{A}$ and $\boldsymbol{B}$; $\mathrm{vec}(\boldsymbol{A})$ is the column vector obtained by stacking the columns of matrix $\boldsymbol{A}$, e.g., if $\boldsymbol{A}=[\boldsymbol{a}_1,\boldsymbol{a}_2]$, $\mathrm{vec}(\boldsymbol{A})=\left[\begin{smallmatrix}\boldsymbol{a}_1\\ \boldsymbol{a}_2\end{smallmatrix}\right]$; and $x\sim\mathcal{CN}(0,\sigma^2)$ means that a complex random variable x conforms to a complex normal distribution with a zero mean and variance σ^2. E[x] stands for the expectation of random variable x.

II. Double STLC Design

We first introduce a 1×2 STLC scheme in [1] with its alternative form, and then design an $M\times 4$ D-STLC scheme that transmits two-data streams through M antennas (precisely, four information symbols, x_1, x_2, x_3, and x_4, through M-transmit antennas in consecutive transmissions).

A. Alternative Form of 1×2 STLC Signal and System Model

Consider a 1×2-STLC system that has one-transmit and two-receive antennas and transmits a single data stream. Two information symbols, x_1 and x_2, are delivered to the Rx through two consecutive transmissions, where without loss of generality $\mathrm{E}[|\mathrm{x_i}|^2]=1$.

Employing a type-five STLC structure in [1, Table 4], the STLC symbols in [1] are alternatively represented as follows:

$$[s_1\quad s_2]=\frac{\sqrt{P}\boldsymbol{h}^H}{\|\boldsymbol{h}\|}\begin{bmatrix}x_1 & -x_2^*\\ x_2 & x_1^*\end{bmatrix},\tag{1}$$

where $\boldsymbol{h}=[h_1,h_2]^T$ is a channel vector and h_n represents the channel gain from the transmit antenna to receive antenna n. Here, the transmit power is assumed to be limited by P i.e., $\mathbb{E}[|s_t|^2]=P$. Denoting $r_{n,t}$ is the received signal at receive antenna n at time t, the received signals for two consecutive time intervals are then expressed as a matrix form, i.e.

$$\boldsymbol{R}=\begin{bmatrix}r_{1,1} & r_{1,2}\\ r_{2,1} & r_{2,2}\end{bmatrix}=[\boldsymbol{r}_1\quad\boldsymbol{r}_2]=\boldsymbol{h}[s_1\quad s_2]+\boldsymbol{Z}\in\mathbb{C}^{2\times 2},\tag{2}$$

where $\boldsymbol{R}\in\mathbb{C}^{2\times 2}$ is the received signal matrix; $\boldsymbol{r}_t\in\mathbb{C}^{2\times 1}$ is the received signal vector at time t; $\boldsymbol{Z}=[\boldsymbol{z}_1\quad\boldsymbol{z}_2]\in\mathbb{C}^{2\times 2}$ is a noise matrix whose (n,t)th element $z_{n,t}$ is the additive white Gaussian noise (AWGN) at $r_{n,t}$. Here, a block fading channel is assumed, such that the channel is static for two symbol durations (i.e., one STLC block) and it varies randomly between STLC blocks.

By stacking $\boldsymbol{r}_1$ on the conjugate of $\boldsymbol{r}_2$, we construct the alternative form of the received signal vector as follows:

$$\begin{aligned}\boldsymbol{r}&=\begin{bmatrix}\boldsymbol{r}_1\\ \boldsymbol{r}_2^*\end{bmatrix}=\begin{bmatrix}r_{1,1}\\ r_{2,1}\\ r_{1,2}^*\\ r_{2,2}^*\end{bmatrix}=\frac{\sqrt{P}}{\|\boldsymbol{h}\|}\begin{bmatrix}h_1h_1^* & h_1h_2^*\\ h_2h_1^* & h_2h_2^*\\ (h_1h_2^*)^* & -(h_1h_1^*)^*\\ (h_2h_2^*)^* & -(h_2h_1^*)^*\end{bmatrix}\begin{bmatrix}x_1\\ x_2\end{bmatrix}+\begin{bmatrix}\boldsymbol{z}_1\\ \boldsymbol{z}_2^*\end{bmatrix}\\ &=\frac{\sqrt{P}}{\|\boldsymbol{h}\|}\begin{bmatrix}\boldsymbol{h}\boldsymbol{h}^H\\ (\boldsymbol{h}\boldsymbol{h}^H)^*\boldsymbol{P}_2\end{bmatrix}\boldsymbol{x}+\boldsymbol{z}\in\mathbb{C}^{4\times 1},\end{aligned}\tag{3}$$

where $\boldsymbol{P}_2=\left[\begin{smallmatrix}0 & -1\\ 1 & 0\end{smallmatrix}\right]$, $\boldsymbol{x}=\left[\begin{smallmatrix}x_1\\ x_2\end{smallmatrix}\right]$, and $\boldsymbol{z}=\left[\begin{smallmatrix}\boldsymbol{z}_1\\ \boldsymbol{z}_2^*\end{smallmatrix}\right]$. Using (3), the combined STLC signals are then represented as follows:

$$\begin{aligned}[\boldsymbol{I}_2\quad\boldsymbol{P}_2^T]\boldsymbol{r}&=\frac{\sqrt{P}}{\|\boldsymbol{h}\|}\left(\boldsymbol{h}\boldsymbol{h}^H+\boldsymbol{P}_2^T(\boldsymbol{h}\boldsymbol{h}^H)^*\boldsymbol{P}_2\right)\boldsymbol{x}+\boldsymbol{z}_1+\boldsymbol{P}_2^T\boldsymbol{z}_2^*\\ &=\sqrt{P}\|\boldsymbol{h}\|\boldsymbol{x}+\boldsymbol{z}_{12}\in\mathbb{C}^{2\times 1},\end{aligned}\tag{4}$$

where $\boldsymbol{z}_{12}=\boldsymbol{z}_1+\boldsymbol{P}_2^T\boldsymbol{z}_2^*$ and $\boldsymbol{z}_{12}\sim\mathcal{CN}(0,2\sigma^2\boldsymbol{I}_2)$. Note that the combining process in (4) does not require CSI and that there is no intersymbol interference (ISI) between x_1 and x_2 in the combined signals. Thus, x_1 and x_2 are recovered using two separate maximum likelihood detections as in an STBC decoder. Here, the effective channel gain $\|\boldsymbol{h}\|$, which is a single real-value scalar, i.e., partial CSI not full CSI, is generally required at the receiver. The effective channel gain can be blindly estimated [21]. For phase-shift keying (PSK) symbol detection, even the partial CSI is not required as it does not affect the phase information. The decoding SNR, ρ_{STLC}, after the STLC combining is readily derived from (4) as

$$\rho_{\mathrm{STLC}}=\frac{P\|\boldsymbol{h}\|^2}{2\sigma^2},\tag{5}$$

which is identical to the decoding SNR of a 2×1 STBC system. From (5), we verify that the 1×2 STLC system achieves the same spatial-diversity and array gains as the 2×1 STBC system, as also verified in [1].

B. Design of $M\times 4$ D-STLC System

Conforming to the alternative structure of 1×2 STLC, we derive an $M\times 4$ D-STLC scheme for $M\geq 2$. Define an STLC symbol transmitted through antenna m at time t by $s_{m,t}$, where $m\in\{1,2,\ldots,M\}$ and $t\in\{1,2\}$. An M-by-2 STLC symbol matrix is then represented as follows:

$$\boldsymbol{S}=\begin{bmatrix}s_{1,1} & s_{1,2}\\ s_{2,1} & s_{2,2}\\ \vdots & \vdots\\ s_{M,1} & s_{M,2}\end{bmatrix}=\frac{\sqrt{P}\boldsymbol{W}}{\|\boldsymbol{W}\|_F}\begin{bmatrix}x_1 & -x_2^*\\ x_2 & x_1^*\\ x_3 & -x_4^*\\ x_4 & x_3^*\end{bmatrix}\in\mathbb{C}^{M\times 2},\tag{6}$$

where $\boldsymbol{W}\in\mathbb{C}^{M\times 4}$ is a general precoding matrix for the D-STLC which we will design. Note that the average transmit power of an $M\times 4$ STLC system is the same as that of a 1×2 STLC system i.e., $\mathrm{E}[\|\boldsymbol{S}\|_{\mathrm{F}}^2]=2\mathrm{P}$. We can interpret that a precoding vector for 1×2 STLC in (1) is the channel vector.

In an $M\times 4$ STLC, the received signals are written in a matrix form as follows:

$$\boldsymbol{R}=[\boldsymbol{r}_1\quad\boldsymbol{r}_2]=\boldsymbol{H}\boldsymbol{S}+\boldsymbol{Z}\in\mathbb{C}^{4\times 2},\tag{7}$$

where $\boldsymbol{r}_t\in\mathbb{C}^{4\times 1}$ is the received signal vector at time t, $\boldsymbol{H}\in\mathbb{C}^{4\times M}$ is the channel matrix whose (n,m)th element $h_{n,m}$ is the channel gain between the mth-transmit and the nth-receive antennas, and $\boldsymbol{Z}\in\mathbb{C}^{4\times 2}$ is the corresponding AWGN matrix to $\boldsymbol{R}$. By stacking $\boldsymbol{r}_1$ on the conjugate of $\boldsymbol{r}_2$ in (7), we now construct the alternative form of the received signal vector $\boldsymbol{r}\in\mathbb{C}^{8\times 1}$ as follows:

$$\boldsymbol{r}=\begin{bmatrix}\boldsymbol{r}_1\\ \boldsymbol{r}_2^*\end{bmatrix}=\frac{\sqrt{P}}{\|\boldsymbol{W}\|_F}\begin{bmatrix}\boldsymbol{H}\boldsymbol{W}\\ (\boldsymbol{H}\boldsymbol{W})^*\boldsymbol{P}_4\end{bmatrix}\boldsymbol{x}+\begin{bmatrix}\boldsymbol{z}_1\\ \boldsymbol{z}_2^*\end{bmatrix},\tag{8}$$

where $\boldsymbol{x}=[x_1\quad x_2\quad x_3\quad x_4]^T$; $\boldsymbol{P}_4=\boldsymbol{I}_2\otimes\boldsymbol{P}_2\in\mathbb{R}^{4\times 4}$; and $\boldsymbol{z}_t\in\mathbb{C}^{4\times 1}$ is the tth column of $\boldsymbol{Z}$. Conforming to the STLC combining structure in (4), the D-STLC received signals in $\boldsymbol{r}$ are simply combined at the Rx as

$$\left[\boldsymbol{I}_4\quad\boldsymbol{P}_4^T\right]\boldsymbol{r}=g\boldsymbol{G}\boldsymbol{x}+\boldsymbol{z}_{12}\in\mathbb{C}^{4\times 1},\tag{9}$$

where $g=\frac{\sqrt{P}}{\|\boldsymbol{W}\|_F}$ is a constant gain, $\boldsymbol{G}=\boldsymbol{H}\boldsymbol{W}+\boldsymbol{P}_4^T\boldsymbol{H}^*\boldsymbol{W}^*\boldsymbol{P}_4$ is an effective channel matrix, and $\boldsymbol{z}_{12}=\boldsymbol{z}_1+\boldsymbol{P}_4^T\boldsymbol{z}_2^*$ with $\boldsymbol{z}_{12}\sim\mathcal{CN}(0,2\sigma^2\boldsymbol{I}_4)$. Since $\boldsymbol{G}\in\mathbb{C}^{4\times 4}$ is clearly a non-diagonal matrix, there exist ISIs among the information symbols $\{x_1,\ldots,x_4\}$. To mitigate the ISI, we design $\boldsymbol{W}$ to minimize the mean-square error (MSE) that is defined as

$$J(\boldsymbol{W}) = \mathrm{E}\left[\|\tilde{\boldsymbol{x}} - \boldsymbol{x}\|^2\right] = \mathrm{E}\left[\left\|\frac{1}{\mathrm{g}}\left[\boldsymbol{I}_4 \quad \boldsymbol{P}_4^{\mathrm{T}}\right]\boldsymbol{r} - \boldsymbol{x}\right\|^2\right], \tag{10}$$

where the partial CSI g is required at the Rx to detect generally modulated symbols, yet it is not required for PSK symbols. Using (10), the optimal $\boldsymbol{W}$ is found as

$$\boldsymbol{W}_o = \min_{\boldsymbol{W}\in\mathbb{C}^{M\times 4}} J(\boldsymbol{W}). \tag{11}$$

From the fact that $J(\boldsymbol{W})$ is a convex function with respect to $\boldsymbol{W}$, we can obtain $\boldsymbol{W}_o$ from the first-order optimality condition, i.e., $\frac{\partial J(\boldsymbol{W})}{\partial \boldsymbol{W}^*} = 0$, which is alternatively written as (see Appendix A for details)

$$\boldsymbol{Q}\boldsymbol{W} + \boldsymbol{H}^H\boldsymbol{P}_4^T\boldsymbol{H}^*\boldsymbol{W}^*\boldsymbol{P}_4 = \boldsymbol{H}^H, \tag{12}$$

where $\boldsymbol{Q} = (\boldsymbol{H}^H\boldsymbol{H} + c\boldsymbol{I}_M)$ and $c = 4\sigma^2/P$.

To obtain $\boldsymbol{W}$ satisfying (12), we rewrite (12) in a vector form as follows:

$$\boldsymbol{A}_1\mathrm{vec}(\boldsymbol{W}) + \boldsymbol{A}_2\mathrm{vec}(\boldsymbol{W}^*) = \mathrm{vec}(\boldsymbol{H}^{\mathrm{H}}) \tag{13}$$

where $\boldsymbol{A}_1 = \boldsymbol{I}_4 \otimes \boldsymbol{Q}$, $\boldsymbol{A}_2 = (\boldsymbol{P}_4 \otimes \boldsymbol{A}_3)$, and $\boldsymbol{A}_3 = \boldsymbol{H}^H\boldsymbol{P}_4\boldsymbol{H}^*$. Equivalently, (13) is rewritten in a vector-matrix form as

$$\begin{bmatrix}\boldsymbol{A}_1 & \boldsymbol{A}_2\\ \boldsymbol{A}_2^* & \boldsymbol{A}_1^*\end{bmatrix}\begin{bmatrix}\mathrm{vec}(\boldsymbol{W})\\ \mathrm{vec}(\boldsymbol{W}^*)\end{bmatrix} = \begin{bmatrix}\mathrm{vec}(\boldsymbol{H}^{\mathrm{H}})\\ \mathrm{vec}(\boldsymbol{H}^{\mathrm{T}})\end{bmatrix}. \tag{14}$$

From the matrix inversion lemma, we obtain

$$\begin{bmatrix}\boldsymbol{A}_1 & \boldsymbol{A}_2\\ \boldsymbol{A}_2^* & \boldsymbol{A}_1^*\end{bmatrix}^{-1} = \begin{bmatrix}\boldsymbol{B}_1 & \boldsymbol{B}_2\\ \boldsymbol{B}_2^* & \boldsymbol{B}_1^*\end{bmatrix}, \tag{15}$$

where $\boldsymbol{B}_1 = (\boldsymbol{A}_1 - \boldsymbol{A}_2(\boldsymbol{A}_1^*)^{-1}\boldsymbol{A}_2^*)^{-1}$ and $\boldsymbol{B}_2 = -\boldsymbol{A}_1^{-1}\boldsymbol{A}_2\boldsymbol{B}_1^*$. Using (15) to (14), $\mathrm{vec}(\boldsymbol{W}_o)$ that satisfies (13) is obtained as

$$\mathrm{vec}(\boldsymbol{W}_o) = \boldsymbol{B}_1\mathrm{vec}(\boldsymbol{H}^{\mathrm{H}}) + \boldsymbol{B}_2\mathrm{vec}(\boldsymbol{H}^{\mathrm{T}}). \tag{16}$$

Using the properties of Kronecker product [22], namely, $(\boldsymbol{A}\otimes\boldsymbol{B})(\boldsymbol{C}\otimes\boldsymbol{D}) = (\boldsymbol{AC})\otimes(\boldsymbol{BD})$ and $(\boldsymbol{B}^T\otimes\boldsymbol{A})\mathrm{vec}(\boldsymbol{X}) = \mathrm{vec}(\boldsymbol{AXB})$, $\mathrm{vec}(\boldsymbol{W}_o)$ in (16) is rewritten in a matrix form, which is the optimal solution of (11), as follows (see Appendix B):

$$\boldsymbol{W}_o = \boldsymbol{C}_1\boldsymbol{H}^H + \boldsymbol{C}_2\boldsymbol{H}^T\boldsymbol{P}_4, \tag{17}$$

where $\boldsymbol{C}_1 = (\boldsymbol{Q} - \boldsymbol{A}_3(\boldsymbol{Q}^*)^{-1}\boldsymbol{A}_3^H)^{-1}$ and $\boldsymbol{C}_2 = \boldsymbol{Q}^{-1}\boldsymbol{A}_3\boldsymbol{C}_1^*$.

C. Analysis on D-STLC Systems

The decoding SINR of D-STLC is derived in Lemma 1.

Lemma 1: The SINR of D-STLC, denoted by ρ_i for x_i, is derived as follows:

$$\rho_i = \frac{P}{4\sigma^2[\boldsymbol{F}]_{i,i}} - 1, i \in \{1,2,3,4\}, \tag{18}$$

where $\boldsymbol{F} = \boldsymbol{H}\boldsymbol{H}^H + \boldsymbol{P}_4^T\boldsymbol{H}^*\boldsymbol{H}^T\boldsymbol{P}_4 + c\boldsymbol{I}_4$ and $[\boldsymbol{F}]_{i,i}$ is the (i,i)th element of $\boldsymbol{F}$.

Proof: See Appendix C. ■

Note that the decoding SINR in (18) is identical to that of a DSTTD system in [17], and this is also verified numerically in Fig. 2, where the decoding SINRs of 2×4 D-STLC, 4×2 DSTTD [17]–[20], 2×4 SM [16], 4×2 precoded STBC [13], and 2×4 STLC [1] are compared over SNR, P/σ^2. Here, the available code rates (denoted by 'cr') for 2×4 STLC are only $3/4$ and $1/2$ i.e., respectively, C5 and C7 in [1, Tab. 7]. It is noticeable that an STLC with full code rate does not exists for four receive antennas as in the STBC system with four transmit antennas.

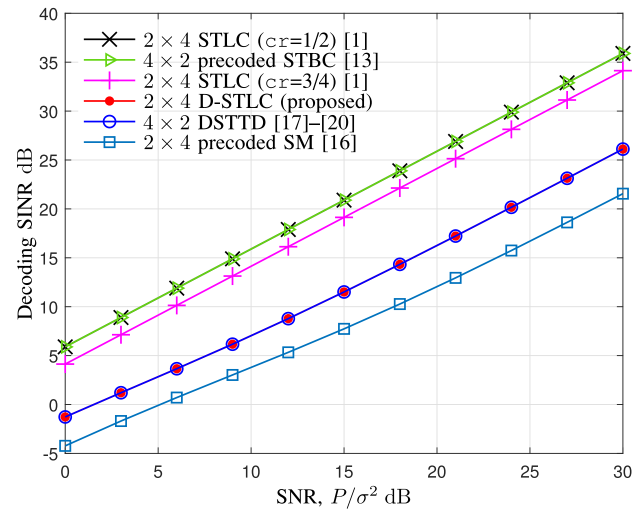

Fig. 2. Decoding SNR comparison of the eight-spatial-channel systems.

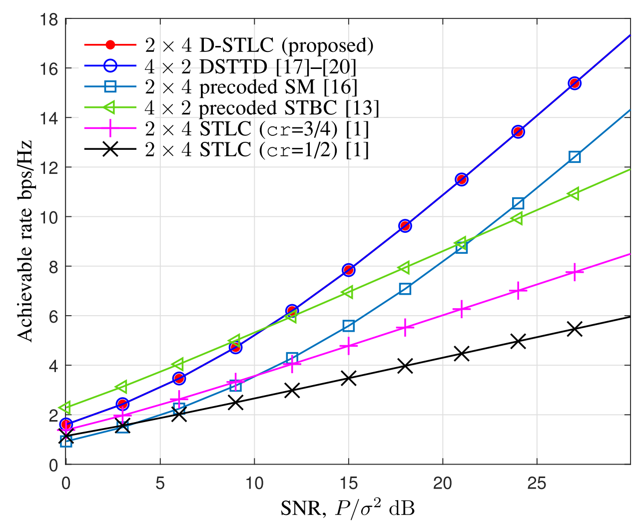

Fig. 3. Achievable rate comparison of the eight-spatial-channel systems.

Since the SINR of D-STLC is the same as that of DSTTD, the diversity order of D-STLC is also identical to that of DSTTD. In a similar approach to [17], the diversity order of the proposed $M\times 4$ D-STLC is obtained in Lemma 2.

Lemma 2: The diversity order of an $M\times 4$ D-STLC system is approximately given by $(2M-2)$ in a high SNR regime.

Proof: See Appendix D. ■

In addition, from (18), the achievable rate of D-STLC is given by

$$\eta = \frac{1}{2}\sum_{i=1}^{4}\log_2(1+\rho_i). \tag{19}$$

In Fig. 3, the achievable rates of the proposed D-STLC, DSTTD [17]–[20], precoded SM [16], precoded STBC [13], and STLC [1] are compared. As shown in the results, the achievable rate of the proposed D-STLC is identical to that of DSTTD and it is significantly greater than that of other schemes, particularly in a high SNR regime. The precoded SM scheme outperforms the conventional STLC scheme, especially, when SNR is high, whereas the precoded STBC outperforms other

TABLE I
MODULATION TYPES AND CODE RATES (cr) FOR $M \times 4$ SYSTEMS WITH FIXED TARGET DATA RATE (dr), WHERE $M \in \{4, 6\}$

Fig.	Data Rate (dr)	1-stream STLC $\mathtt{cr} = 0.5$	Precoded STBC $\mathtt{cr} = 1$	Proposed D-STLC $\mathtt{cr} = 2$	Precoded SM $\mathtt{cr} = 4$
Fig. 4	4 bps/Hz	256-QAM	16-QAM	QPSK	BPSK
Fig. 5	6 bps/Hz	4096-QAM	64-QAM	8-QAM	–
Fig. 6	8 bps/Hz	–	256-QAM	16-QAM	QPSK

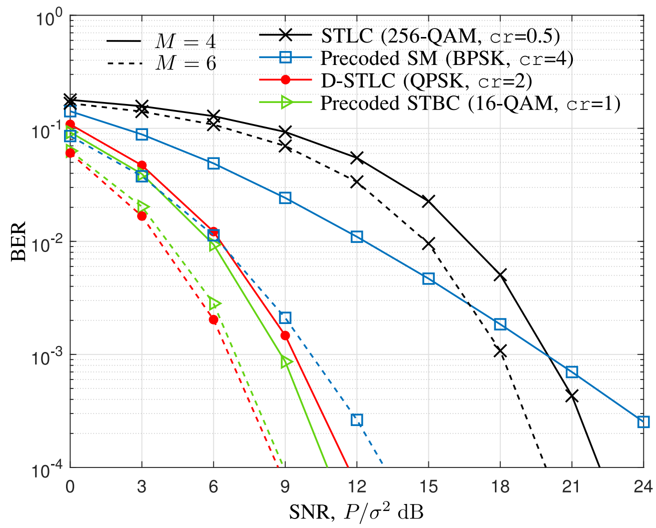

Fig. 4. BER performance comparison of $M \times 4$ systems when $\mathtt{dr} =$ 4 bps/Hz.

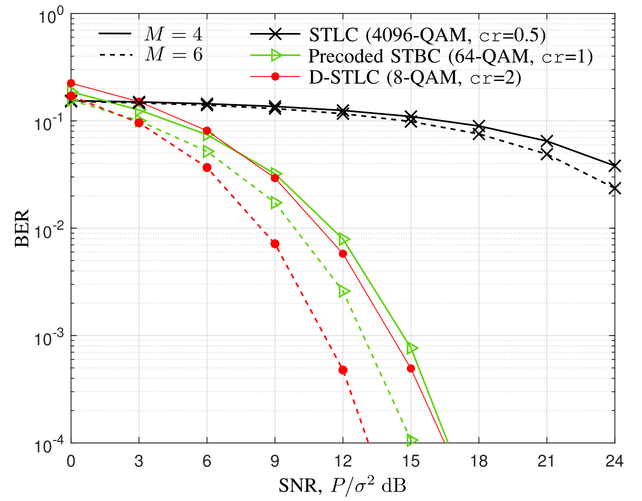

Fig. 5. BER performance comparison of $M \times 4$ systems when $\mathtt{dr} = 6$ bps/Hz.

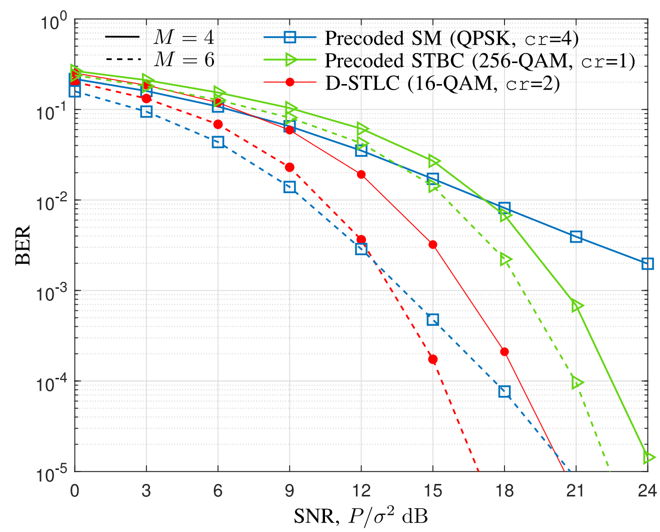

Fig. 6. BER performance comparison of $M \times 4$ systems when $\mathtt{dr} = 8$ bps/Hz.

schemes when SNR is low. Here, note that the precoded STBC uses full CSI at both Tx and Rx. Since the multiplexing schemes, namely D-STLC, DSTTD, and precoded SM, can transmit double data streams, even though their SINRs are lower than that of precoded STBC and STLC schemes as shown in Fig. 2, they can achieve greater rate when SNR is high. This is further verified in the next section through Monte Carlo BER simulation.

III. BER PERFORMANCE EVALUATION AND COMPARISON

In this section, we compare the BER performance of $M \times 4$ systems including STLC, precoded STBC, the proposed D-STLC, and precoded SM, by varying SNR, P/σ^2, where $M \in \{4, 6\}$. Note that the performance of $4 \times M$ DSTTD is omitted in the results since it is identical to that of $M \times 4$ D-STLC. For a fair comparison, we set the target data rates (denoted by 'dr') to be identical for all transmission methods by employing different modulation types and code rates, as summarized in Table I. For specific data rates, namely 4, 6, and 8 bps/Hz, different modulation types, e.g., quadrature amplitude modulation (QAM) and PSK, and the code rates $\mathtt{cr} \in \{0.5, 1, 2, 4\}$ are used for the different schemes.

In Fig. 4, BERs are evaluated for $\mathtt{dr} = 4$. From the simulation results, it is verified that the proposed D-STLC outperforms the conventional single-stream STLC scheme irrespective of the SNR, since the STLC has to employ much higher-order modulation to achieve the same data rate as the D-STLC. The proposed D-STLC also outperforms the SM scheme, since the gain of the precoded SM is marginal when the modulation sizes are similar to each other, namely BPSK for SM and QPSK for D-STLC. On the other hand, D-STLC shows comparable performance to the precoded STBC i.e. D-STLC achieves slightly worse performance than the precoded STBC when $M = 4$; however, it slightly outperforms the precoded STBC when $M = 6$. Here, it is worth reemphasizing that the precoded STBC requires full CSI at both Tx and Rx, whereas D-STLC requires full and partial CSIs at Tx and Rx, respectively. However, as the data rate increases to $\mathtt{dr} = 6$, the D-STLC scheme outperforms the precoded STBC regardless of M and SNR, as shown in Fig. 5. This is further clearly shown as the data rate increases to $\mathtt{dr} = 8$ as shown in Fig. 6. For the high data rate, i.e., $\mathtt{dr} = 8$, the precoded SM slightly outperforms D-STLC in the low SNR region, due to the high multiplexing gain. However, with large spatial-diversity gain, the proposed D-STLC outperforms others when SNR is greater than 7.5 dB for $M = 4$ and 12.5 dB for $M = 6$.

From the results, we can surmise that the proposed D-STLC is generally a promising spatial diversity-and-multiplexing scheme, particularly in a high-SNR regime.

IV. CONCLUSION

In this paper, a D-STLC that transmits two-STLC data streams has been designed for a system with M-transmit and four-receive antennas with full CSI only at the transmitter. It has been shown that the spatial-diversity and spatial-multiplexing gains of an $M \times 4$ D-STLC are identical to those of a $4 \times M$ DSTTD that transmits two STBC data streams. Through numerical simulations, it has been verified that the achievable rate and BER performance can be dramatically improved by using the proposed D-STLC, especially when the SNR and/or data rate is high. The proposed $M \times 4$ D-STLC scheme can be directly extended to an arbitrary number of the receive antennas. Moreover, it is a good research topic to combine conventional high-rate STBCs with the STLC transmission scheme.

Appendix A
First Order Optimality Condition in (12)

Proof: From the definition of MSE in (10), we can write

$$\begin{aligned}
J(\boldsymbol{W}) &= \mathrm{E}\left[\left\|\left(\boldsymbol{H}\boldsymbol{W} + \boldsymbol{P}_4^T\boldsymbol{H}^*\boldsymbol{W}^*\boldsymbol{P}_4\right)\boldsymbol{x} + g^{-1}\boldsymbol{z}_{12} - \boldsymbol{x}\right\|^2\right] \\
&= \mathrm{E}\left[\left\|\left(\boldsymbol{H}\boldsymbol{W} + \boldsymbol{P}_4^T\boldsymbol{H}^*\boldsymbol{W}^*\boldsymbol{P}_4 - \boldsymbol{I}_4\right)\boldsymbol{x} + g^{-1}\boldsymbol{z}_{12}\right\|^2\right] \\
&= \mathrm{tr}\left[\left(\boldsymbol{W}^H\boldsymbol{H}^H + \boldsymbol{P}_4^H\boldsymbol{W}^T\boldsymbol{H}^T\boldsymbol{P}_4 - \boldsymbol{I}_4\right)\mathrm{E}[\boldsymbol{x}\boldsymbol{x}^H]\right. \\
&\quad \left.\times \left(\boldsymbol{H}\boldsymbol{W} + \boldsymbol{P}_4^T\boldsymbol{H}^*\boldsymbol{W}^*\boldsymbol{P}_4 - \boldsymbol{I}_4\right)\right] + g^{-2}\mathrm{E}\left[\boldsymbol{z}_{12}^H\boldsymbol{z}_{12}\right] \\
&= \mathrm{tr}\left[\left(\boldsymbol{W}^H\boldsymbol{H}^H + \boldsymbol{P}_4^H\boldsymbol{W}^T\boldsymbol{H}^T\boldsymbol{P}_4 - \boldsymbol{I}_4\right)\right. \\
&\quad \left.\times \left(\boldsymbol{H}\boldsymbol{W} + \boldsymbol{P}_4^T\boldsymbol{H}^*\boldsymbol{W}^*\boldsymbol{P}_4 - \boldsymbol{I}_4\right)\right] + 2c\,\mathrm{tr}\left(\boldsymbol{W}\boldsymbol{W}^H\right)
\end{aligned}$$

where we used that $\mathrm{tr}(\boldsymbol{A}\boldsymbol{B}) = \mathrm{tr}(\boldsymbol{B}\boldsymbol{A})$, $\boldsymbol{P}_4^T = -\boldsymbol{P}_4$, and $\boldsymbol{P}_4\boldsymbol{P}_4{}^T = \boldsymbol{I}_4$. The first derivative of $J(\boldsymbol{W})$ with respect to $\boldsymbol{W}^*$ is then derived as follows:

$$\frac{\partial J(\boldsymbol{W})}{\partial \boldsymbol{W}^*} = 2\boldsymbol{H}^H\boldsymbol{H}\boldsymbol{W} + 2\boldsymbol{H}^H\boldsymbol{P}_4^T\boldsymbol{H}^*\boldsymbol{W}^*\boldsymbol{P}_4 - 2\boldsymbol{H}^H + 2c\boldsymbol{W}.$$

Therefore, the condition, $\frac{\partial J(\boldsymbol{W})}{\partial \boldsymbol{W}^*} = 0$, is equivalent to (12). This completes the proof. ∎

Appendix B
Derivation of (17)

Proof: We first represent $\boldsymbol{B}_1$ as follows:

$$\begin{aligned}
\boldsymbol{B}_1 &= \left[\boldsymbol{I}_4 \otimes \boldsymbol{Q} - (\boldsymbol{P}_4 \otimes \boldsymbol{A}_3)\left(\boldsymbol{I}_4 \otimes (\boldsymbol{Q}^*)^{-1}\right)(\boldsymbol{P}_4 \otimes \boldsymbol{A}_3^*)\right]^{-1} \\
&= \left[\boldsymbol{I}_4 \otimes \boldsymbol{Q} - (\boldsymbol{P}_4\boldsymbol{I}_4\boldsymbol{P}_4) \otimes \boldsymbol{A}_3(\boldsymbol{Q}^*)^{-1}\boldsymbol{A}_3^*\right]^{-1} \\
&= \left[\boldsymbol{I}_4 \otimes \boldsymbol{Q} + \boldsymbol{I}_4 \otimes \boldsymbol{A}_3(\boldsymbol{Q}^*)^{-1}\boldsymbol{A}_3^*\right]^{-1} \\
&= \left[\boldsymbol{I}_4 \otimes \left(\boldsymbol{Q} + \boldsymbol{A}_3(\boldsymbol{Q}^*)^{-1}\boldsymbol{A}_3^*\right)\right]^{-1} \\
&= \boldsymbol{I}_4 \otimes \left[\boldsymbol{Q} - \boldsymbol{A}_3(\boldsymbol{Q}^*)^{-1}\boldsymbol{A}_3^H\right]^{-1} \\
&= \boldsymbol{I}_4 \otimes \boldsymbol{C}_1. \qquad \text{(B.1)}
\end{aligned}$$

Here, we used that $(\boldsymbol{A} \otimes \boldsymbol{B})(\boldsymbol{C} \otimes \boldsymbol{D}) = (\boldsymbol{A}\boldsymbol{C}) \otimes (\boldsymbol{B}\boldsymbol{D})$, $(\boldsymbol{I} \otimes \boldsymbol{A} + \boldsymbol{I} \otimes \boldsymbol{B}) = \boldsymbol{I} \otimes (\boldsymbol{A} + \boldsymbol{B})$, $\boldsymbol{P}_4^T = -\boldsymbol{P}_4$, $\boldsymbol{P}_4\boldsymbol{P}_4{}^T = \boldsymbol{I}_4$, and $\boldsymbol{A}_3^* = -\boldsymbol{A}_3^H$.

By substituting (B.1) to (16), the optimal vector, $\mathrm{vec}(\boldsymbol{W}_{\mathrm{o}})$, is the further derived as follows:

$$\begin{aligned}
\mathrm{vec}(\boldsymbol{W}_{\mathrm{o}}) &= (\boldsymbol{I}_4 \otimes \boldsymbol{C}_1)\,\mathrm{vec}(\boldsymbol{H}^{\mathrm{H}}) - (\boldsymbol{I}_4 \otimes \boldsymbol{Q})^{-1} \\
&\qquad \times (\boldsymbol{P}_4 \otimes \boldsymbol{A}_3)(\boldsymbol{I}_4 \otimes \boldsymbol{C}_1)^*\mathrm{vec}(\boldsymbol{H}^{\mathrm{T}}) \\
&= \mathrm{vec}(\boldsymbol{C}_1\boldsymbol{H}^{\mathrm{H}}) - (\boldsymbol{I}_4\boldsymbol{P}_4\boldsymbol{I}_4) \otimes \left(\boldsymbol{Q}^{-1}\boldsymbol{A}_3\boldsymbol{C}_1^*\right) \\
&\qquad \times \mathrm{vec}(\boldsymbol{H}^{\mathrm{T}}) \\
&= \mathrm{vec}(\boldsymbol{C}_1\boldsymbol{H}^{\mathrm{H}}) - \boldsymbol{P}_4 \otimes \left(\boldsymbol{Q}^{-1}\boldsymbol{A}_3\boldsymbol{C}_1^*\right)\mathrm{vec}(\boldsymbol{H}^{\mathrm{T}}) \\
&= \mathrm{vec}(\boldsymbol{C}_1\boldsymbol{H}^{\mathrm{H}}) - \mathrm{vec}\left(\boldsymbol{Q}^{-1}\boldsymbol{A}_3\boldsymbol{C}_1^*\boldsymbol{H}^{\mathrm{T}}\boldsymbol{P}_4^{\mathrm{T}}\right) \\
&= \mathrm{vec}\left(\boldsymbol{C}_1\boldsymbol{H}^{\mathrm{H}} + \boldsymbol{Q}^{-1}\boldsymbol{A}_3\boldsymbol{C}_1^*\boldsymbol{H}^{\mathrm{T}}\boldsymbol{P}_4\right), \qquad \text{(B.2)}
\end{aligned}$$

where we used that $(\boldsymbol{A} \otimes \boldsymbol{B})^{-1} = \boldsymbol{A}^{-1} \otimes \boldsymbol{B}^{-1}$, $(\boldsymbol{A} \otimes \boldsymbol{B})(\boldsymbol{C} \otimes \boldsymbol{D}) = (\boldsymbol{A}\boldsymbol{C}) \otimes (\boldsymbol{B}\boldsymbol{D})$ and $(\boldsymbol{B}^T \otimes \boldsymbol{A})\mathrm{vec}(\boldsymbol{X}) = \mathrm{vec}(\boldsymbol{A}\boldsymbol{X}\boldsymbol{B})$. By reconstructing the vectors in (B.2) into a matrix form, we obtain (17). This completes the proof. ∎

Appendix C
Proof of SINR in Lemma 1

Proof: Suppose that $\boldsymbol{W}_o$ in (17) is used at the transmitter. From (8) and (9), the decoding error vector is given by

$$\boldsymbol{e}_o = \left(\begin{bmatrix}\boldsymbol{H} & \boldsymbol{P}_4^T\boldsymbol{H}^*\end{bmatrix}\begin{bmatrix}\boldsymbol{W}_o \\ \boldsymbol{W}_o^*\boldsymbol{P}_4\end{bmatrix} - \boldsymbol{I}_4\right)\boldsymbol{x} + g^{-1}\boldsymbol{z}_{12}. \qquad \text{(C.1)}$$

We first derive the correlation matrix of $\boldsymbol{e}_o$ as follows:

$$\begin{aligned}
\boldsymbol{R}_e &= E[\boldsymbol{e}_o\boldsymbol{e}_o^H] \\
&= \boldsymbol{I}_4 - \begin{bmatrix}\boldsymbol{H} & \boldsymbol{P}_4^T\boldsymbol{H}^*\end{bmatrix}\begin{bmatrix}\boldsymbol{W}_o \\ \boldsymbol{W}_o^*\boldsymbol{P}_4\end{bmatrix}, \qquad \text{(C.2)}
\end{aligned}$$

where the first-order optimality condition in (12) was used. The correlation matrix is rewritten as

$$\begin{aligned}
\boldsymbol{R}_e &= \boldsymbol{I}_4 - \begin{bmatrix}\boldsymbol{H} & \boldsymbol{P}_4^T\boldsymbol{H}^*\end{bmatrix}\begin{bmatrix}\boldsymbol{C}_1\boldsymbol{H}^H + \boldsymbol{C}_2\boldsymbol{H}^T\boldsymbol{P}_4 \\ \boldsymbol{C}_2^*\boldsymbol{H}^H + \boldsymbol{C}_1^*\boldsymbol{H}^T\boldsymbol{P}_4\end{bmatrix} \\
&= \boldsymbol{I}_4 - \begin{bmatrix}\boldsymbol{H} & \boldsymbol{P}_4^T\boldsymbol{H}^*\end{bmatrix}\begin{bmatrix}\boldsymbol{C}_1 & \boldsymbol{C}_2 \\ -\boldsymbol{C}_2^* & \boldsymbol{C}_1^*\end{bmatrix}\begin{bmatrix}\boldsymbol{H}^H \\ \boldsymbol{H}^T\boldsymbol{P}_4\end{bmatrix} \\
&\overset{(a)}{=} \boldsymbol{I}_4 - \boldsymbol{H}_t\left(\boldsymbol{H}_t^H\boldsymbol{H}_t + c\boldsymbol{I}_{2M}\right)^{-1}\boldsymbol{H}_t^H \\
&\overset{(b)}{=} c(\boldsymbol{H}_t\boldsymbol{H}_t^H + c\boldsymbol{I}_4)^{-1} = c\boldsymbol{F}^{-1}, \qquad \text{(C.3)}
\end{aligned}$$

where $\boldsymbol{H}_t = [\boldsymbol{H}\ \boldsymbol{P}_4^T\boldsymbol{H}^*] \in \mathbb{C}^{4\times 2M}$; (a) follows the fact that

$$\begin{aligned}
\left(\boldsymbol{H}_t^H\boldsymbol{H}_t + c\boldsymbol{I}_{2M}\right)^{-1} &= \begin{bmatrix}\boldsymbol{H}^H\boldsymbol{H} + c\boldsymbol{I}_M & \boldsymbol{H}^H\boldsymbol{P}_4^T\boldsymbol{H}^* \\ \boldsymbol{H}^T\boldsymbol{P}_4\boldsymbol{H} & \boldsymbol{H}^T\boldsymbol{H}^* + c\boldsymbol{I}_M\end{bmatrix}^{-1} \\
&= \begin{bmatrix}\boldsymbol{Q} & -\boldsymbol{A}_3 \\ -\boldsymbol{A}_3^H & \boldsymbol{Q}^*\end{bmatrix}^{-1} = \begin{bmatrix}\boldsymbol{C}_1 & \boldsymbol{C}_2 \\ -\boldsymbol{C}_2^* & \boldsymbol{C}_1^*\end{bmatrix}; \qquad \text{(C.4)}
\end{aligned}$$

and (b) is obtained from the matrix inversion lemma. Since the (i, i)th element of $\boldsymbol{R}_e$ is the MSE for decoding x_i, the decoding SINR of D-STLC is expressed as (18). ∎

Appendix D
Proof of Diversity Order in Lemma 2

Proof: From (16), $\boldsymbol{W}_o$ is rewritten as

$$\boldsymbol{W}_o = [\boldsymbol{C}\quad \boldsymbol{F}][\boldsymbol{g}_1\quad \boldsymbol{g}_2\quad \boldsymbol{g}_3\quad \boldsymbol{g}_4] \qquad \text{(D.1)}$$

where $[\boldsymbol{g}_1\ \boldsymbol{g}_2\ \boldsymbol{g}_3\ \boldsymbol{g}_4] = \left[\begin{smallmatrix}\boldsymbol{H}^H \\ \boldsymbol{H}^T\boldsymbol{P}_4\end{smallmatrix}\right]$ for $\boldsymbol{g}_i \in \mathbb{C}^{2M\times 1}$. Since $\boldsymbol{g}_1^H\boldsymbol{g}_2 = \boldsymbol{g}_3^H\boldsymbol{g}_4 = 0$, from (12) of [17], the decoding SINR values for symbols

$\{x_1, x_2, x_3, x_4\}$ can be described as

$$\rho_1 = \boldsymbol{g}_1^H \left(\boldsymbol{g}_3\boldsymbol{g}_3^H + \boldsymbol{g}_4\boldsymbol{g}_4^H + c\boldsymbol{I}_4\right)^{-1} \boldsymbol{g}_1, \tag{D.2}$$

$$\rho_2 = \boldsymbol{g}_2^H \left(\boldsymbol{g}_3\boldsymbol{g}_3^H + \boldsymbol{g}_4\boldsymbol{g}_4^H + c\boldsymbol{I}_4\right)^{-1} \boldsymbol{g}_2, \tag{D.3}$$

$$\rho_3 = \boldsymbol{g}_3^H \left(\boldsymbol{g}_1\boldsymbol{g}_1^H + \boldsymbol{g}_2\boldsymbol{g}_2^H + c\boldsymbol{I}_4\right)^{-1} \boldsymbol{g}_3, \tag{D.4}$$

$$\rho_4 = \boldsymbol{g}_4^H \left(\boldsymbol{g}_1\boldsymbol{g}_1^H + \boldsymbol{g}_2\boldsymbol{g}_2^H + c\boldsymbol{I}_4\right)^{-1} \boldsymbol{g}_4. \tag{D.5}$$

In (D.2), all decoded symbols have the same diversity order because the SINR expressions have the same structure. Without loss of generality, we consider the decoding SINR ρ_1 only. By eigen decomposition, we can write

$$\boldsymbol{g}_3\boldsymbol{g}_3^H + \boldsymbol{g}_4\boldsymbol{g}_4^H = \boldsymbol{U}\boldsymbol{\Lambda}\boldsymbol{U}^H \tag{D.6}$$

where $\boldsymbol{U} \in \mathbb{C}^{2M\times 2\,M}$ is a unitary matrix and $\boldsymbol{\Lambda} = \mathrm{diag}(\lambda_1, \lambda_2, 0, \ldots, 0) \in \mathbb{R}^{2M\times 2\,M}$ with eigenvalues λ_1 and λ_2. Using (D.6), we can rewrite ρ_1 as follows:

$$\begin{aligned}\rho_1 &= \boldsymbol{g}_1^H\boldsymbol{U}(\boldsymbol{\Lambda} + c\boldsymbol{I}_4)^{-1}\boldsymbol{U}^H\boldsymbol{g}_1 \\ &= \boldsymbol{v}^H(\boldsymbol{\Lambda} + c\boldsymbol{I}_4)^{-1}\boldsymbol{v} \\ &= \frac{|v_1|^2}{\lambda_1 + c} + \frac{|v_2|^2}{\lambda_2 + c} + \frac{1}{c}\sum_{i=3}^{2M}|v_i|^2,\end{aligned} \tag{D.7}$$

where $\boldsymbol{v} = \boldsymbol{U}^H\boldsymbol{g}_1 \in \mathbb{C}^{2M\times 1}$ and v_i is the ith element of $\boldsymbol{v}$. In high SNR region, $\lambda_1 = \lambda_2 = \|\boldsymbol{g}_1\|^2 = \|\boldsymbol{g}_2\|^2 \gg c = \frac{4\sigma^2}{P}$, and thus, we can approximate the SINR ρ_1 as

$$\rho_1 \approx \frac{1}{c}\left(|v_3|^2 + |v_4|^2 + \cdots + |v_{2\,M}|^2\right). \tag{D.8}$$

Notice that the distribution of $|v_i|^2$ is identical to that of $|h_{n,m}|^2$ from the definitions of $\boldsymbol{g}_1$ and $\boldsymbol{v}$, and that the approximated SINR expressions for ρ_2, ρ_3, and ρ_4 can be dirived in a similar form to ρ_1. Therefore, the diversity order of the proposed D-STLC is approximately $2M - 2$ for all data streams in high SNR region. ■

REFERENCES

[1] J. Joung, "Space–time line code," *IEEE Access*, vol. 6, pp. 1023–1041, 2018.

[2] S. M. Alamouti, "A simple transmitter diversity technique for wireless communications," *IEEE J. Sel. Areas Commun.*, vol. 16, no. 8, pp. 1451–1458, Oct. 1998.

[3] V. Tarokh, H. Jafarkhani, and A. R. Calderbank, "Space–time block codes from orthogonal designs," *IEEE Trans. Inf. Theory*, vol. 45, no. 5, pp. 1459–1467, Jul. 1999.

[4] D. Lee, "Symbol error rate analysis of scheduled STBC with power allocation in CR-MIMO systems," *IEEE Trans. Veh. Technol.*, vol. 67, no. 7, pp. 6218–6228, Jul. 2018.

[5] A. F. Coşkun and O. Kucur, "Secrecy outage probability of conventional and modified TAS/Alamouti-STBC schemes with power allocation in the presence of feedback errors," *IEEE Trans. Veh. Technol.*, vol. 68, no. 3, pp. 2609–2623, Mar. 2019.

[6] J. Joung, "Space–time line code for massive MIMO and multiuser systems with antenna allocation," *IEEE Access*, vol. 6, pp. 962–979, 2018.

[7] J. Joung and E.-R. Jeong, "Multiuser space-time line code with optimal and suboptimal power allocation methods," *IEEE Access*, vol. 6, pp. 51766–51775, 2018.

[8] J. Joung, "Energy efficient space-time line coded regenerative two-way relay under per-antenna power constraints," *IEEE Access*, vol. 6, pp. 47 026–47 035, 2018.

[9] J. Joung and J. Choi, "Space-time line code with power allocation for regenerative two-way relay systems," *IEEE Trans. Veh. Technol.*, vol. 68, no. 5, pp. 4884–4893, May 2019.

[10] J. Joung and J. Choi, "Uneven power amplifier shuffling for space-time line code (STLC) systems," *IEEE Access*, vol. 6, pp. 58491–58500, 2018.

[11] J. Joung and B. C. Jung, "Machine learning based blind decoding for space-time line code (STLC) systems," *IEEE Trans. Veh. Technol.*, vol. 68, no. 5, pp. 5154–5158, May 2019.

[12] J. Joung, J. Choi, B. C. Jung, and S. Yu, "Artificial noise injection and its power loading methods for secure space-time line coded systems," *MDPI Entropy*, vol. 21, no. 5, pp. 1–12, May 2019.

[13] D. J. Love and R. W. Heath, Jr., "Limited feedback unitary precoding for orthogonal space-time block codes," *IEEE Trans. Signal Process.*, vol. 53, no. 1, pp. 64–73, Jan. 2005.

[14] G. Jöngren, M. Skoglund, and B. Ottersten, "Combining beamforming and orthogonal space–time block coding," *IEEE Trans. Inf. Theory*, vol. 48, no. 3, pp. 611–627, Mar. 2002.

[15] M. Bhatnagar and A. Hjørungnes, "Linear precoding of STBC over correlated Rician MIMO channels," *IEEE Trans. Wireless Commun.*, vol. 9, no. 6, pp. 1832–1836, Jun. 2010.

[16] T. Haustein, C. von Helmolt, E. Jorswieck, V. Jungnickel, and V. Pohl, "Performance of MIMO systems with channel inversion," in *Proc. IEEE Veh. Technol. Conf.*, May 2002, vol. 1, pp. 35–39.

[17] J. Wu, Y. R. Zheng, A. Gumaste, and C. Xiao, "Error performance of double space time transmit diversity system," *IEEE Trans. Wireless Commun.*, vol. 6, no. 9, pp. 3191–3196, Sep. 2007.

[18] Y. Lee and H. Shieh, "A simple layered space-time block nulling technique for DSTTD systems," *IEEE Commun. Lett.*, vol. 15, no. 12, pp. 1323–1325, Dec. 2011.

[19] M. C. Park, B. G. Jo, and D. S. Han, "Double space-time transmit diversity with spatial modulation," *IET Elect. Lett.*, vol. 51, no. 25, pp. 2155–2156, Dec. 2015.

[20] M. Le, T. Nguyen, X. Tran, and V. Ngo, "On the combination of double space time transmit diversity with spatial modulation," *IEEE Trans. Wireless Commun.*, vol. 17, no. 1, pp. 170–181, Jan. 2018.

[21] P. Gao and C. Tepedelenlioglu, "SNR estimation for nonconstant modulus constellations," *IEEE Trans. Signal Process.*, vol. 53, no. 3, pp. 865–870, Mar. 2005.

[22] D. A. Harville, *Matrix Algebra From a Statistician's Perspective*, 1st ed. New York, NY, USA: Springer-Verlag, 1997.

[23] S. Haykin, *Digital Communication Systems*. Hoboken, NJ, USA: Wiley, 2014.